

Effects of air transient spark discharge and helium plasma jet on water, bacteria, cells, and biomolecules

Karol Hensel,^{a)} Katarína Kučerová, Barbora Tarabová, Mário Janda, and Zdenko Machala
Faculty of Mathematics, Physics and Informatics, Comenius University, 84248 Bratislava, Slovakia

Kaori Sano

Department of Environmental and Life Sciences, Toyohashi University of Technology, 4418580 Toyohashi, Japan

Cosmin Teodor Mihai, Mitiță Ciortac, and Lucian Dragos Gorgan

Faculty of Biology, Alexandru Ioan Cuza University, 700506 Iași, Romania

Roxana Jijie, Valentin Pohoata, and Ionut Topala

Faculty of Physics, Alexandru Ioan Cuza University, 700506 Iași, Romania

(Received 16 March 2015; accepted 21 April 2015; published 6 May 2015)

Atmospheric pressure DC-driven self-pulsing transient spark (TS) discharge operated in air and pulse-driven dielectric barrier discharge plasma jet (PJ) operated in helium in contact with water solutions were used for inducing chemical effects in water solutions, and the treatment of bacteria (*Escherichia coli*), mammalian cells (*Vero* line normal cells, *HeLa* line cancerous cells), deoxyribonucleic acid (*dsDNA*), and protein (*bovine serum albumin*). Two different methods of water solution supply were used in the TS: water electrode system and water spray system. The effects of both TS systems and the PJ were compared, as well as a direct exposure of the solution to the discharge with an indirect exposure to the discharge activated gas flow. The chemical analysis of water solutions was performed by using colorimetric methods of UV-VIS absorption spectrophotometry. The bactericidal effects of the discharges on bacteria were evaluated by standard microbiological plate count method. Viability, apoptosis and cell cycle were assessed in normal and cancerous cells. Viability of cells was evaluated by trypan blue exclusion test, apoptosis by Annexin V-FITC/propidium iodide assay, and cell cycle progression by propidium iodide/RNase test. The effect of the discharges on deoxyribonucleic acid and protein were evaluated by fluorescence and UV absorption spectroscopy. The results of bacterial and mammalian cell viability, apoptosis, and cell cycle clearly show that cold plasma can inactivate bacteria and selectively target cancerous cells, which is very important for possible future development of new plasma therapeutic strategies in biomedicine. The authors found that all investigated bio-effects were stronger with the air TS discharge than with the He PJ, even in indirect exposure. © 2015 American Vacuum Society. [<http://dx.doi.org/10.1116/1.4919559>]

I. INTRODUCTION

A large number of recent publications on various biomedical applications of nonthermal (cold) atmospheric pressure plasmas demonstrate a fast evolution and a great potential of this new interdisciplinary field. Thanks to ionizations, dissociations, excitations, production of chemically active species and reactions occurring at relatively low gas temperatures, the cold plasma bio-decontamination and sterilization has been well established over the last 15 years. It is evident that cold plasmas can efficiently kill various microbes, even highly resistant forms such as bacterial spores and biofilms, making cold plasmas are very suitable for disinfection and sterilization of surfaces, medical instruments, water, air, food, and even living tissues.¹⁻³ Various cold plasma sources have also been proven to induce interesting phenomena in the cells of higher organisms, often leading to promising therapeutic effects when carefully set and dosed. However,

despite numerous reported positive effects of plasma disinfection and therapeutic treatments, plasma interaction with living cells and microorganisms still remains not well understood and the plasma treatment of biomolecules, cells, and tissues is still a subject of debate.³⁻⁵

The first reported plasma treatments of mammalian cells was probably nondestructive manipulation of mammalian cells by plasma leading to cell detachment from each other and from the substrate in a reversible manner.⁶ Later, the possibility of plasma-induced apoptosis in mammalian cells has been described.⁷ Unlike necrosis, which is a premature cell death caused by traumatic external factors, apoptosis or “programmed cell death” is a form of physiologic cell death and a normal way of disposing of damaged or nonfunctional cells in high organisms. Apoptosis is induced in response to a variety of cellular stress factors including toxins, oxidative stress, or DNA damage. Induction of apoptosis is one of the therapeutic approaches for cancer treatment.⁸ The possibility to inactivate tumor cells via induction of apoptosis by atmospheric-pressure plasma treatment in vitro was

^{a)}Electronic mail: hensel@fmph.uniba.sk

demonstrated repeatedly.^{9–11} The initial hypothesis that plasma-induced apoptosis is triggered by plasma-generated reactive oxygen species (ROS)⁷ was proved by several experimental studies using a variety of plasma sources. Other experimental studies give rise to the assumption that at least some types of cancerous cells are more sensitive to plasma-induced inactivation compared to normal cells.^{11,12}

Most plasma sources considered for direct biological and medical applications have the following characteristics: the contribution of electrode surfaces to the discharge production is negligible, only strong volume ionization takes place; and the plasma is confined to a discharge channel of small diameter. It is difficult to generate large volume plasmas at atmospheric pressure with parameters that will meet all criteria for medical devices proposed for direct use in contact with tissues: low or no thermal effects, nontoxic chemical effects, and electricity and UV radiations limits. Reaction channels induced by plasma in aqueous solutions and biological fluids, as well as post treatment chemical dynamics in biological environment need to be studied in detail in order to better understand the mechanisms of plasma-cell and plasma-tissue interactions, which would provide information allowing standardized medical treatments and direct clinical uses of atmospheric pressure cold plasma sources.

From molecular point of view, cells may be regarded as complex supramolecular assemblies, stabilized by short range interactions. The plasma agents (e.g., photons, electric field, charged particles, and radicals) have individual or synergic effects on all biomolecular systems. In order to induce a specific biological effect using single or repeated plasma exposure it is necessary to explore all reaction channels that can be triggered by the plasma action, including here not only simple physical or chemical damage to biomolecules but also soft structural modifications, and changes of biological environment, e.g., acidification or local reactive oxygen and nitrogen species (RONS) balance shift. Many studies have investigated the effects of cold atmospheric plasmas to biomolecules up to now. In general, plasma treatment of lipids results in lipid peroxidation, with implications to changes of cell membrane fluidity, integrity and transport.^{13–15} A lot of attention has been devoted to plasma treatment of amino acids and proteins, resulting typically in oxidations and structural changes of amino acids and protein denaturation.^{16–21} Even DNA and RNA have been subjected to plasma treatments, with the observed effects such as double strand breaks and fragmentation.^{22–25} DNA inactivation is mainly caused by plasma-generated RONS, especially long-lived species, such as organic peroxides generated in the liquid cell environment.¹¹

Cancer and its associated disorders is one of the most spread diseases nowadays, with a high impact on the life quality, health budgets, and a great emotional impact to the relatives. A major problem of the current therapeutic strategies for cancer treatment is the lack of major efficiency followed by relapse of cancer due to acquired drug resistance. Today, there is a dire need for novel cancer therapeutics and

combination strategies that could efficiently overcome current treatment limitations.²⁶ The main studies regarding the effects of cold atmospheric plasmas on different types of cancerous cells showed that cold plasma can induce apoptosis^{10,12,27–32} and cell cycle arrest,^{33,34} by generation of RONS. Both types of reactive species induce a direct effect on cells and also act as intracellular signaling triggers.³⁵ In addition, an important feature of cold atmospheric plasmas is their selectivity for cancerous cell targets with a reduced damaging impact on normal cells.^{11,35–39} This trait is a “must have” of the oncolytic therapy, the nonselectivity of the current therapeutics and the side effects being limiting factors of the effectiveness. By increasing number of the cancerous cells in the S phase of the cell cycle, their susceptibility to the cold plasmas or another cytostatic action is higher, allowing for a possible destruction of a larger population of cancerous cells.³³ Cold plasmas have been reported to induce the detachment of cancerous cells from the extracellular matrix, decrease migration velocity of cancerous cells,⁴⁰ stimulate the immune function and migration of immune cells,⁴¹ modulate the blood flow and the tissue oxygen partial pressure creating the conditions toward tumor blood vessel normalization⁴² and inhibition of the metastatic processes.²⁹ From this point of view, cold plasma is a new and promising alternative agent for classical oncology therapies both as a single or associative agent of the current oncochemotherapeutics.^{27,43–45}

The most commonly used and studied plasma discharges at atmospheric pressure are coronas and dielectric barrier discharges easily operated in air, and plasma jets typically operated in noble gases and blown into the air.^{46,47} The apparent advantage of air plasmas is using the ambient atmosphere as an operating gas, providing very easy and cheap implementation. In addition, air is a precursor of RONS generated in the plasma that turn out to be very important in biomedical applications.^{48,49} Numerous studies have shown the importance of RONS in biological systems, from the inactivation of bacteria^{50,51} to the intricacies of cell signaling pathways.⁵² The disadvantage of air discharges is a self-pulsing character and relatively easy transition to arc. However, the pulsing character can be beneficial for repetitive production of reactive species and radiation without losing too much energy for undesirable gas heating. Arcing can be prevented or controlled by using dielectric barriers (typical for dielectric barrier discharges) or electrical circuit limiting the current or the discharged energy. One example of limiting the discharge energy to avoid the plasma thermalization and excessive gas heating, while taking advantage of very reactive pulsing streamer and streamer-to-spark transition environment in atmospheric air is the transient spark (TS): a dc-driven self-pulsing discharge with high current pulses of extremely short duration (~ 10 – 100 ns) and the typical repetition frequency of 1–10 kHz. TS, originally reported as prevented spark,⁵³ is initiated by a streamer transforming to a short spark current pulse. Streamers are considered to be crucial for the efficiency of plasma induced chemistry at atmospheric pressure, since the electric field in

the streamer's head reaches more than 200 kV/cm (Ref. 54) allowing for the very efficient chemical and ionization processes. The TS has been successfully tested for multiple biological and environmental applications, such as bio-decontamination of water, lean flame stabilization, or exhaust gas cleaning.^{14,55}

Atmospheric pressure plasma jet refers to a family of plasma sources, driven by alternative high voltage with frequency in kHz or MHz range or by high voltage pulses usually of ns to ms duration. Dielectric tubes, with internal or external electrodes, host a flow of working gas (e.g., helium, argon with optional oxygen, nitrogen, or water impurities), and present millimeters or even centimeters long plasma channels, of jet type appearance,⁵⁶ blown out into the open atmosphere. These plasma sources are relatively easy to handle, show a gas temperature near to room temperature, and their great advantage is that the active plasma is ejected outside from the interelectrode area. This secures no direct physical contact of the treated target with the high voltage electrodes, minimizing the possibility of electric shock and allows for driving the plasma in long tubes.⁵⁷ Despite no contact of the target with the high voltage electrodes, an electrical connection between them still exists. The propagating plasma channel transports the intense electric field and creates charged and neutral species and UV photons on the target. The propagation of the plasma ionization front and its consecutive recombination is affected by the presence of the target when compared to the free jet propagation. One possible way to generate plasma without direct contact from the HV electrode to the target may be achieved by combination of perpendicularly set capillary tubes, where the plasma generated in one tube is capable to generate secondary ionization wave in another spatially separated and electrodeless tube by so called plasma transfer phenomenon.^{58,59} For these advantages, plasma jets are being extensively investigated and tested for many biomedical applications in direct contact with living cells^{9,60,61} and tissues, e.g., for skin and wound sterilization,^{62–65} or cancer treatment.^{33,66–68}

The objective of this paper is to demonstrate some effects of cold plasmas on bacteria, eukaryotic cells, and selected biomolecules that are related to bio-decontamination and potential cancer therapies. Furthermore, we compare the direct and indirect effects of two different cold atmospheric plasma sources: the self-pulsing transient spark discharge generated in air as an efficient producer of RONS applicable for water solutions and biomolecules, and the pulsed dielectric barrier discharge (DBD) plasma jet (PJ) generated in helium as a representative of the most convenient plasma sources for direct cell/tissue treatments and medical *in-vivo* applications. We investigate the interaction of the discharges with water solutions containing bacteria, normal and cancerous cells and selected biomolecules (DNA, protein). Chemical effects induced by the discharges were investigated and linked to the biophysical response of bacteria (*Escherichia coli*), monkey kidney epithelial cells (Vero) and human cervix epithelioid carcinoma cells (HeLa), and the effect on DNA and protein (bovine serum albumin).

Direct exposure of the water solutions to the plasma was compared with an indirect exposure of the solutions to the plasma activated gas flow.

We are well aware that simple comparison of direct treatment by air plasma streamer-to-spark discharge with the plasma effluent of the He DBD plasma jet is impossible, since they are completely different plasma sources with different electrical and gas parameters. Nevertheless, from the point of view of the effects induced on specific targets (water solutions, bacteria, mammalian cells, DNA and protein) such comparison can stress out the important plasma agents and parameters of the plasma sources used that are crucial for achieving the specific effect. From this target-effect perspective, we can suggest that a specific plasma source that causes substantially stronger effects (of course without damaging the target) is obviously more suitable for the specific application.

II. EXPERIMENT

A. Discharge systems

1. Air transient spark discharge

The first type of the discharge we used in the experiments is the positive DC-driven TS discharge, a repetitive streamer-to-spark transition discharge generated in ambient air, described in detail in Refs. 55, 69, and 70. The discharge was generated in ambient air in two different configurations: the water electrode systems and the water-spray systems. The water electrode (WE) system, depicted in Fig. 1(a), consisted of high voltage hollow needle electrode placed above the inclined grounded plane electrode in point-to-plane geometry. In this system, the water solution was supplied via a narrow channel in the plane electrode and circulated by a peristaltic pump with a constant flow rate (14 ml/min).

The water spray (WS) system, depicted in Fig. 1(b) and described in detail in Ref. 71 consisted of high voltage hollow needle electrode placed above the grounded mesh electrode also in point-to-plane geometry. The water solution was supplied via the needle with a constant flow rate (0.5 ml/min). Thanks to the applied high voltage the solution was electrospayed through the active zone of the discharge and then collected under the metallic mesh.

The chemical and biological effects of the direct discharge action on water solutions were investigated and compared to the indirect exposure to discharge activated gas flow using the setup depicted in Fig. 1(c). The setup was similar to Fig. 1(b), but instead of supplying the solution via the discharge zone, the sample (water solution) was placed 1–2 mm under the grounded mesh electrode. The hollow needle electrode was used to supply additional gas flow to drive neutral active species generated by the discharge toward the sample. The sample in this case was a phosphate-buffered saline (PBS) solution of cells in well plates, each well plate containing 100 μ l PBS to prevent cell drying.

All three TS systems (WE, WS, and indirect system) were operated in ambient atmospheric pressure air with the interelectrode distance of 1 cm. Positive DC high voltage

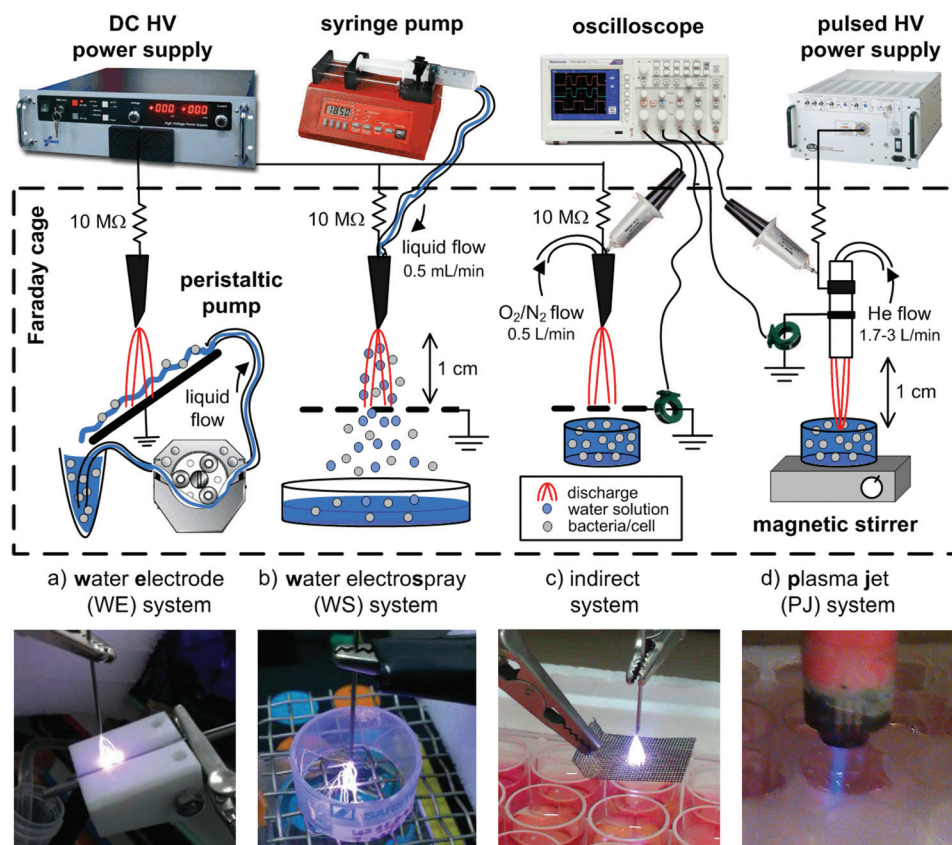


Fig. 1. Experimental systems of the TS in WE and WS configurations for direct plasma exposure; TS for indirect exposure to the plasma activated gas flow and the system of the PJ. The reference photographs of the individual discharges are shown.

(HV) was applied through the ballast resistor R ($10\text{ M}\Omega$) to maintain the TS mode operating in the following typical conditions: generator voltage $\sim 12\text{--}16\text{ kV}$, spark pulse repetition frequency $\sim 1\text{--}4\text{ kHz}$, and exposure time up to 20 min. Treated volume of water was $2\text{--}5\text{ ml}$ (for direct exposure) and $100\ \mu\text{l}$ (for indirect exposure). In the direct TS exposure, several milliliters of collected solution was necessary in order to perform all relevant chemical and biological analysis. In the case of indirect TS, due to its smaller chemical activity where direct discharge contact is supplemented by discharge activated flow of active species toward the solution, much smaller volume of $100\ \mu\text{l}$ was used instead. The discharge voltage signal was measured by the HV probe (*Tektronix P6015A*), the discharge current signal was measured on $1\ \Omega$ resistor or by current monitor (*Pearson 2877*) while both signals were processed by the oscilloscope (*Tektronix TDS 2024*).

2. He plasma jet

The second discharge type used in the experiments is positive pulse-driven DBD PJ generated in atmospheric pressure helium, and depicted in Fig. 1(d). The device consists of a quartz cylindrical tube (inner diameter 4 mm, outer diameter 6 mm, and length 7 cm) with two aluminum tape electrodes (10 mm width for the high voltage electrode and 4 mm for the ground electrode) wrapped around the external surface of

the tube. A 10 mm gap was fixed between the electrodes and 7 mm between the quartz tube tip and the first electrode (ground). The system was operated with helium flow rate of $1.7\text{--}3\text{ l/min}$. The PJ was excited using high voltage pulses delivered by a high voltage amplifier (*Trek PD07016*) and a digital waveform generator (*Tektronix AFG3022B*). Positive high voltage pulses with amplitudes $\sim 3\text{--}9\text{ kV}$ and frequencies $\sim 1\text{--}8\text{ kHz}$ were applied on the high voltage electrode. The exposure time was $3\text{--}10\text{ min}$ and was adjusted to be similar to the one used for indirect TS due to the common character of the two treatments (effect of discharge activated gas flow). The plasma generated between the electrodes expanded into the open air atmosphere forming a jet with a typical length of few centimeters and a diameter of a few millimeters. The distance between the jet nozzle and the treated sample (surface of the liquid) was kept constant at 1 cm. The applied voltage and discharge current waveforms were monitored and stored using a high voltage probe (*Tektronix P6015A*) and a current probe (*Pearson 6485*) connected to a digital oscilloscope (*Tektronix TDS5034*).

B. Measurements of chemical effects induced in water

Comprehensive studies on chemical environment generated in water solutions during plasma exposure are essential in order to understand the plasmas effects on biological samples during direct or indirect exposure. Water solutions with

different initial pH and electrolytic conductivities σ were used for plasma exposure. The solutions were prepared by the dissolution of different salts in deionized water:

- (1) **deionized water** (pH 5.5 and $\sigma = 1\text{--}2 \mu\text{S/cm}$)
- (2) **“water”** (pH 5–5.5 and $\sigma = 0.6 \text{ mS/cm}$)—solution of $\text{Na}_2\text{H}_2\text{PO}_4$ in deionized water that mimics the conductivity of tap water and has chemical composition similar to the phosphate buffer but no buffering capacity
- (3) **saline** (pH 6.7 and $\sigma = 6.35 \text{ mS/cm}$)—solutions of NaCl salt in deionized water
- (4) **PB** (pH 6.9 and $\sigma = 0.56 \text{ mS/cm}$) and **PBS** (pH 6.9 and $\sigma = 5.95 \text{ mS/cm}$)—solutions of $\text{Na}_2\text{HPO}_4/\text{KH}_2\text{PO}_4$ buffer in deionized water and saline solution, respectively, represent the buffered counterparts to ‘water’ and saline solutions.

RONS generated by the discharge plasma in treated water solutions were detected mostly by colorimetric methods using UV/VIS absorption spectrometry (*Shimadzu UV-1700*) and fluorescence spectroscopy. In general, we measure aqueous concentrations of H_2O_2 , NO_2^- , NO_3^- , ONOO^- , and O_3 in the treated solutions,⁷¹ however here we do present only the results on H_2O_2 and NO_2^- as example to demonstrate the chemical potential of the TS and its comparison with the PJ.

- (1) Hydrogen peroxide (H_2O_2) was measured by titanium sulfate colorimetric method with the absorption maximum 407 nm. The method is independent of the pH since the measurement of H_2O_2 is performed in strongly acidic solution of sulfuric acid. In the presence of nitrites (NO_2^-), the solution of sodium azide NaN_3 was added to the samples prior to mixing with titanium sulfate reagent to eliminate decomposition of H_2O_2 by NO_2^- under acidic conditions.
- (2) Nitrites (NO_2^-) were measured by the reaction with Griess reagents (*Cayman Chemical Nitrate/Nitrite Colorimetric Assay Kit*) resulting into formation of azo-dye with the absorption maximum at 540 nm. The results obtained using Griess reagents were verified by the measurements of NO_2^- concentration by ion chromatography (*Shimadzu LC-Avp with UV 210 nm*) and suppressed conductivity detection. All treated samples for ion chromatography analysis were fixed by buffer to stop the acidic decomposition of nitrites.

C. Measurements of bactericidal effects

Bactericidal effects of the studied plasma discharges were tested on Gram-negative bacteria *E. coli* (CCM3954) suspended in deionized water in planktonic form with initial populations from 10^7 to 10^8 colony forming units per ml (CFU ml^{-1}). The microbial cultivation was carried out in a sterile environment in the following steps: an overnight bacterial culture was prepared in a shaker with sterile liquid nutrient. They were then centrifuged several times and diluted in “water”/saline solutions to obtain desired concentrations. The plasma experiments with bacteria suspensions were performed with the TS in both WS and WE systems and replicated 10–15 times. The bactericidal tests with the PJ were

repeated up to three times. The number of bacteria cells in the suspension was evaluated by counting colony forming units (CFUs) cultivated on agar plates (*MFC, HiMedia, Mumbai, India, and Biolab*) during 12–24 h at 37 °C. Several tenfold dilution series were used to achieve optimum number of CFUs grown on agar plates (30–300), especially for controls and low inactivation rates. For high inactivation rates of plasma treated water no dilutions were needed. Usually, three to four agar plates from each sample were taken for statistical evaluation. The viability of bacteria was determined as the ratio of the population of surviving bacteria in plasma treated samples to the total population in reference samples.

D. Measurements of mammalian cell viability and apoptosis

The HeLa (human cervix epithelioid carcinoma) and Vero (monkey kidney epithelial cells) cells were grown in Dulbecco’s modified Eagle’s medium, supplemented with 10% fetal bovine serum, 100 $\mu\text{g/ml}$ streptomycin, and 100 IU/ml penicillin. The cell culture reagents were purchased from *Biochrom AG*. In the case of direct TS exposure, the cells were seeded at a density of 3×10^5 cells/flask in 25 m^2 flasks, while in the case of indirect TS and PJ exposure, the cells were seeded at the density of 5×10^4 cells/well in 100 μL wells (*TPP Techno Plastic Products AG*). The cells were maintained in a CO_2 incubator (*Binder CB 150*) at 37 °C with 5% CO_2 and 95% humidified atmosphere and allowed to divide for 24 h to attain the log stage. Before the direct TS exposure, the cells were detached by trypsinization and resuspended in 5 mL of PBS to set the initial concentration to 5×10^5 cells/mL. In the case of indirect TS and PJ exposure, the culture media in wells was only replaced by 100 μL of PBS to keep the same initial concentration to 5×10^5 cells/mL. After the plasma exposure in all TS and PJ systems, the cells were centrifuged to discard PBS, covered with culture medium and allowed to recover for 4 or 24 h. After the incubation, the cells were detached by trypsinization, resuspended in culture medium, centrifuged, resuspended in PBS, stained with different fluorochromes and finally analyzed.

Viability of the cells exposed to the plasma was determined by trypan blue exclusion test using a Turk hemocytometer,⁷² while apoptosis was assessed with Annexin V-FITC/propidium iodide kit (*eBioscience*). For the apoptotic evaluation, the cells were harvested by trypsinization and washed twice with cold PBS. After the final wash the cell pellet was resuspended in binding buffer (provided with the kit) and stained successively with Annexin V-FITC and propidium iodide. After 30 min of incubation in dark, the samples were immediately analyzed by flow cytometer (*Beckman Coulter CellLab Quanta SC*) using blue laser for excitation and fluorescence was collected for FITC using 525 nm bandpass filter and for PI using 670 nm long pass filter.

For cell cycle analysis, the cell suspension was pipetted in cold 70% ethanol and incubated overnight at –20 °C. The ethanol permeabilizes the cell membranes, while low temperature preserves the cell integrity. After ethanol was

discarded by centrifugation, cell pellet was suspended in staining solution (propidium iodide, RNase A, Triton X-100), incubated for 40 min at 37 °C, pelleted and suspended in PBS for analysis on flow cytometer (*Beckman Coulter CellLab Quanta SC*) using blue laser for excitation and fluorescence was collected using 670 nm long pass filter.

E. Measurements of effect on biomolecules

Tests of plasma exposure on various biomolecules, including dsDNA (double strand deoxyribonucleic acid) and protein (bovine serum albumin) were performed. UV absorption spectroscopy and fluorescence spectroscopy were used to quantify the DNA damage and the protein inactivation (conformation changes) caused by the plasma exposure.

The DNA used in the experiments was isolated from muscle tissue of *Bison bonasus* using the Wizard Genomic DNA Purification Kit (*Promega*) according to the producer specifications. The total DNA was eluted and both reference and treated samples were quantified (ng/ μ l) with ACTGene absorption spectrophotometer, before and after plasma exposure in order to estimate the degree of DNA integrity. The solutions used in the experiments contained 9 ng/ μ l of DNA in 2 ml of deionized water. An amount of tDNA previously isolated, was subjected to PCR using a specific primers pair for cytochrome b gene (approximately 1140 bp), followed by purification step using Wizard SV Gel and PCR Clean Up System (*Promega*). The obtained amplicons solution was divided into unexposed samples (reference) and exposed samples (plasma treated). For each sample, the amount of double strand DNA was estimated

using average fluorescence emitted by SYBR Green fluorochrome (*Corbett RotorGene 6000*). DNA-dye-complex absorbs light at 497 nm and emits light at 520 nm.

Protein solution of 3–4 ml was prepared from a 1 mg/ml stock solution of bovine serum albumin (BSA, *Sigma Aldrich A4503–5G*). In the case of the PJ exposure, the BSA solution was gently stirred at about 25 °C. After the plasma treatment, the BSA structural modification was monitored using fluorescence measurements. Intrinsic fluorescence of native and plasma modified BSA was carried out using a double monochromator spectrofluorometer (*SLM Instruments SLM 8000*) with an excitation wavelength of 280 nm and maximum fluorescence intensity at 345 nm. Although the protein possesses a natural absorption band at 268 nm, the UV absorption spectroscopy was not used to determine its concentration, as the species produced by the plasma in the water solution masked the UV spectra in the region below 350 nm.

III. RESULTS AND DISCUSSION

A. Discharge systems

Two different cold atmospheric plasma sources were used and tested in this study for their chemical, biocidal and cytotoxic effects—the self-pulsing TS generated in air and the DBD PJ generated in helium.

1. Air transient spark discharge

Electrical and optical characteristics of the TS operating in atmospheric air were published in detail in our previous works.^{69–71} The typical voltage and current waveforms of

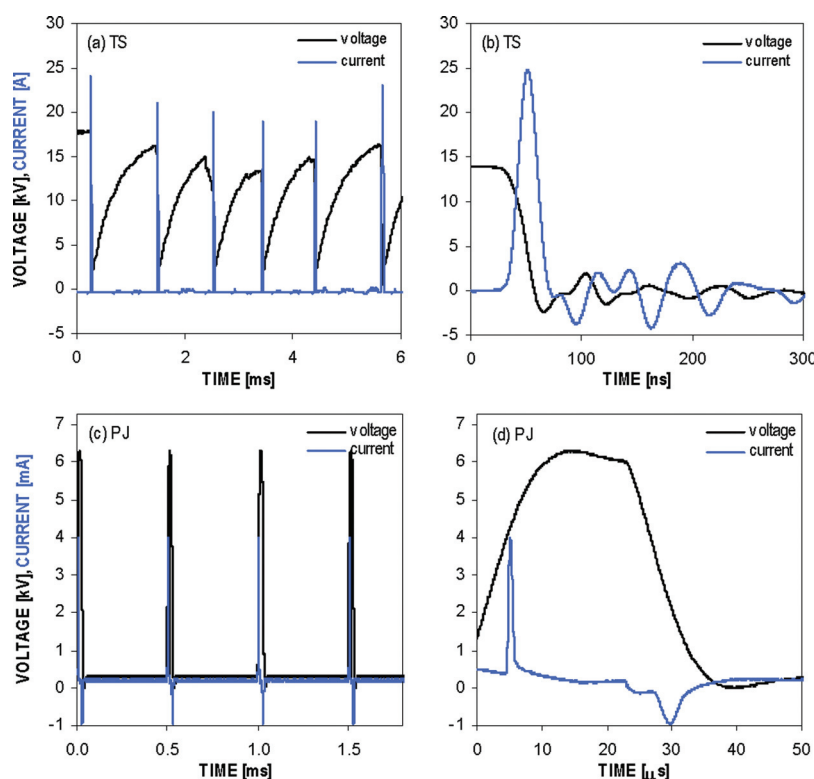


FIG. 2. Typical current and voltage waveforms of the TS in air [(a) and (b)] and the PJ in helium [(c) and (d)] in different time scales.

the positive TS discharge in 1 cm gap with electrospray of water are shown in Figs. 2(a) and 2(b) in two different time scales. When a positive high voltage of a few kV is applied to the point electrode streamer corona appears. With further increase of the voltage (up to ~ 12 kV), the streamers establish a conductive channel that leads to a spark breakdown with excessive current pulse. During the spark, the internal circuit capacity C (in our case of order of 10 pF) discharges completely and the potential V on the HV electrode drops to almost zero. Thus, when the sparks forms, it is only transient since the energy discharged from C is small. Due to the very short spark current pulse duration (≈ 10 – 100 ns) and small amount of dissipated energy, the plasma could not reach equilibrium conditions.⁷⁰ After the spark, the potential V starts to gradually increase as the capacity C recharges. The TS becomes then a self-pulsing repetitive streamer-to-spark transition discharge with spark pulses (≈ 10 A) preceded by one or a sequence of streamer pulses. The repetitive frequency of the TS is usually 0.5–10 kHz and it can be well controlled by the increasing applied voltage. The amplitude of TS current pulses depends on the internal capacity C , TS repetition frequency, and the breakdown voltage (determined mostly by the distance between the electrodes d). The current pulses amplitude increases with increasing C and d , while the increasing TS repetition frequency has the opposite effect. The smaller and broader pulses at higher TS frequencies are related to the gas preheating and decrease of the breakdown voltage with growing frequency.^{69,70} For $d = 1$ cm, $C \sim 35$ pF, and $f \sim 1$ kHz, the current pulse amplitude can be as high as ~ 25 A [Figs. 2(a) and 2(b)].

In case of water solutions electrosprayed through the TS discharge zone (WS), a great care was taken to keep the constant electrical parameters throughout each experiment since the water substantially perturbed the discharge regularity (especially the pulse frequency), while in the WE system the discharge was affected by the regularity of water flow driven by the peristaltic pump. In order to keep the constant power dissipated into the discharge, water flows were adjusted carefully (0.5 ml/min for the WS, and 14 ml/min for the WE) to obtain highly repeatable discharge pulses with the almost regular frequency. In addition, the radius of curvature of the needle deteriorated in time, which influenced the streamer formation and subsequent streamer-to-spark transition that is essential in this discharge mechanism. In order to keep the constant power dissipated into the discharge, the pulse frequency was controlled at the given frequency. The typical applied average power of the TS used in this work was 1–4 W, with energy 1–4 mJ per pulse. Optical emission spectroscopy confirmed nonthermal character and high reactivity of TS plasma.^{70,73,74} The emission of excited atomic radicals (O^* , N^*), molecules N_2^* and ions N_2^{+*} was observed and the electron density as high as 10^{17} cm⁻³ was determined.

2. He plasma jet

Electrical parameters, discharge dynamics, and emission spectra of the PJ were presented in detail in previous

TABLE I. Typical electrical parameters of the TS in air and the PJ in helium.

	Transient spark	Plasma jet
Applied voltage	12–16 kV	3–9 kV
Current pulse amplitude I_{\max}	~ 10 A	1–10 mA
Current pulse duration	~ 10 ns	~ 1 μ s
Current pulse frequency	1–4 kHz	2–8 kHz
Mean current I_{mean}	0.1–1 mA	1–10 μ A
Mean power P_{mean}	1–4 W	2–20 mW
Energy in a single pulse	1–4 mJ/pulse	25–50 μ J/pulse

works.^{75–77} Distinct current pulses of mA order amplitude and microsecond duration [Figs. 2(c) and 2(d)] appeared during each increasing and decreasing edge of the applied high voltage signal. The typical applied average power of the PJ was 2–20 mW, and depended on the applied voltage in the range of 3–9 kV. The average power per pulse was equal to 1–2.5 W and the energy 25–50 μ J per pulse. With no target facing the PJ, an apparently continuous plasma channel of a length of few centimeter and a diameter ~ 2 – 3 mm was generated. The summary of the typical electrical parameters of both the PJ and the TS are presented side-by-side in Table I.

In the case of the PJ, a great care was also taken to minimize the effect of water target placed in the front of the jet. The water electrolyte acts as a conductive tagret and collected some electrical current during each discharge pulse. Nevertheless, the electrical current intensity is strongly affected by the distance between the plasma generation region (i.e., electrodes region) and the water surface. The 10 mm distance used in this study was selected in order to minimize the electrical current effect and to still have a plasma channel with acceptable dimensions. No other parameters (i.e., frequency and power) were affected by the presence of water solution in front of plasma channel.

High speed camera imaging enabled us to gain more information on the plasma temporal dynamics. Localized plasma structures (so called “plasma bullets”) are generated in different spatial positions, and the apparent propagation velocity of these bullets is being of the order of 10^5 m/s. Any tagret facing the plasma jet is exposed to these bullets, assuring a different, pulsed, reaction environment in comparison with continuous wave plasmas. The analysis of the light emitted by the PJ demonstrated the presence of helium lines along with lines and bands of air impurities: atomic oxygen, neutral and ionized molecular nitrogen, and hydroxyl radical. Although the fast helium flow rate assures the formation of a long gas channel outside the quartz tube, impurities penetrate the channel and then plasma electrons mediate processes such as dissociation and excitation. The gas temperature in the PJ was estimated using a Boltzmann plot analysis of rotational spectra corresponding to molecular nitrogen positive ion, using a method reliable for neon and helium DBD discharges.⁷⁸ The temperatures of ~ 350 K were estimated for the external jet facing the tagret. Recent results have shown that exploitation of barrier discharge principles and the use of capillary dielectric tubes allowed the design and operation of a very low volume plasma source able to induce controllable effects on proteins and amino acids.⁷⁹

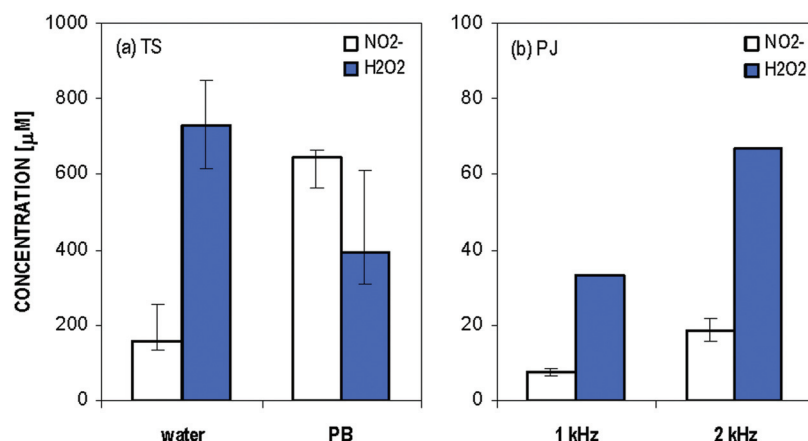


FIG. 3. Typical concentration of H_2O_2 and NO_2^- generated in water and PB solutions after plasma exposure to the TS and the PJ systems: (a) TS WS system in water and PBS solutions [sample volume 5 ml, applied voltage ~ 12 kV, frequency ~ 1 kHz, exposure time 10 min], (b) PJ system with frequency of 1 and 2 kHz [water, sample volume 2 ml, He gas flow rate 1.7 l/min, applied voltage ~ 9 kV, exposure time 5 min].

B. Chemical effects induced in water

The TS discharge was generated in ambient air at atmospheric pressure in the direct contact with treated water solutions or in the indirect contact where samples were exposed to plasma activated gas flow. In direct plasma treatment, it was shown that the bactericidal effects on bacterial suspensions were accompanied with the decrease of pH, increase of solution conductivity and the chemical changes in water solutions, i.e., formation of various RONS: H_2O , NO_2^- , NO_3^- , O_3 , and ONOO^- .⁷¹ Figure 3(a) shows typical concentration of H_2O_2 , and NO_2^- as determined in water and PB solutions after treatment by the WS system. The concentration of other active species generated in the same conditions as those presented in Fig. 3(a) were as follows: NO_3^- (900–1000 μM ; analyzed after enzymatic conversion to NO_2^- by Griess reagents), ozone (negligible; analyzed by phenol chemical probe⁸⁰). The aqueous species measured in WS and WE systems showed very similar concentrations.

In general, gas-phase plasma generated by the TS in contact with liquid efficiently produces nitrogen oxides NO_x and hydroxyl OH radicals. Upon entering the water solution, OH radicals produce hydrogen peroxide H_2O_2 , while NO_x dissolve and form NO_2^- , NO_3^- responsible for the acidification of the treated solution. Under acidic conditions the subsequent decay of NO_2^- may happen either via the reaction with H_2O or H_2O_2 . The first one leads to an increase of NO_3^- concentration, the second one into formation of peroxyntrous acid $\text{O}=\text{NOOH}$ or its conjugate base peroxyntrite $\text{O}=\text{NOO}^-$.^{71,80} Peroxyntrites are relatively strong oxidants with a large bactericidal effect that may significantly contribute to the cytotoxic effect induced by air plasma in water, as proposed by several researchers.^{71,80,81} Under acidic conditions, their bactericidal effect is determined mainly by OH^\bullet and NO_2^\bullet radicals formed during the decomposition reaction of peroxyntrous acid.⁸⁰ Therefore, we can hypothesize that the so called acidified nitrites possess strong and often long-term bactericidal properties due to the peroxyntrite chemistry.^{48,51}

The comparison of the concentrations of selected RONS generated by the TS in air [Fig. 3(a)] and the PJ in helium [Fig.

3(b)] shows that the concentrations generated by the TS were much higher than those generated by the PJ system. Relatively low concentrations of the active species generated in water and overall limited plasma chemical activity of the PJ subsequently resulted in its limited bactericidal and cytotoxic effects toward the cells, as shown in Secs. III C and III D.

C. Bactericidal effects

E. coli suspended in nonbuffered and buffered water solutions with different initial pH and electrolytic conductivity were treated by TS discharge. The bactericidal efficiency expressed as a logarithmic reduction is depicted in Fig. 4. In both TS WE and WS systems, the stronger bactericidal effect was observed in nonbuffered water solution (3–5 log) than in PB solutions (1–2 log). In the WS system, the efficiency was slightly higher than in the WE system. This was probably due to the effect of the electro-spray, where the treated water solution is sprayed to micrometric size droplets, which enhances the surface-to-volume ratio and thus the mass transfer of RONS formed in the gas phase into the solution. The higher efficiency observed in nonbuffered solutions was linked with the different RONS chemistry

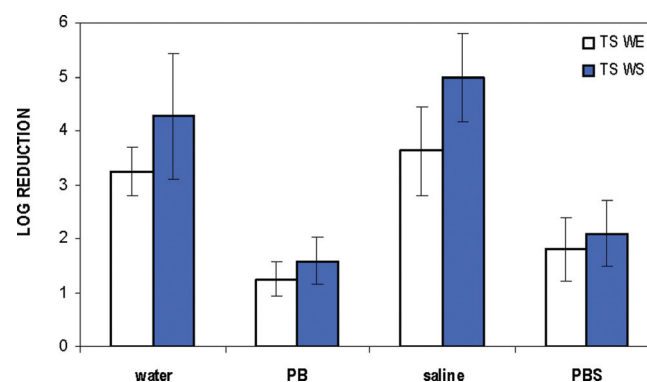


FIG. 4. Bactericidal effect of direct exposure on *E. coli* to the TS discharge in the WE system [liquid volume 5 ml, liquid flow rate 14 ml/min, exposure time 10 min] and the WS system [liquid volume 5 ml, liquid flow rate 0.5 ml/min, exposure time 10 min].

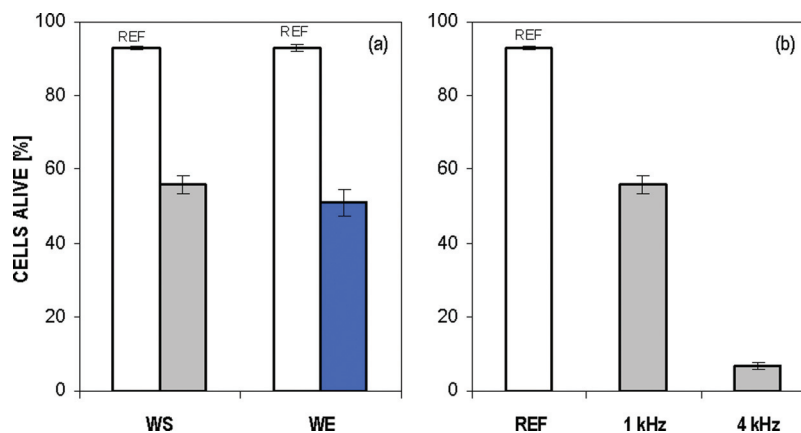


FIG. 5. Viability of **HeLa** line cells after direct exposure to the TS discharge: (a) comparison of **WS** and **WE** systems efficiency [cells in PBS, sample volume 5 ml, frequency ~ 1 kHz, exposure time 10 min], (b) effect of discharge frequency in **WS** system [frequency 1 and 4 kHz, exposure time 10 min].

associated with acidification (down to $pH \sim 3$) and increase of the conductivity ($0.6 \rightarrow 0.8$ mS/cm; $6 \rightarrow 6.5$ mS/cm) observed in both systems. In PB and PBS solutions, the bactericidal efficiency was lower with almost no decrease of pH and very low increase of conductivity, which showed the important role of pH in plasma induced bactericidal effects.⁷¹

The bactericidal effect of the PJ in water solutions was also tested. In the same conditions as those presented in Fig. 3(b), a fair log reduction < 1 was usually observed. It is the result of a limited chemical activity of the PJ and generation of much lower concentrations of the active species in water solutions than in the TS as shown in Fig. 3.

D. Effects on mammalian cells

This chapter presents the main results of direct and indirect plasma exposure of mammalian cells to the air TS discharge and the He PJ. Viability, apoptosis, and cell cycle of both normal and cancerous cells were assessed.

1. Cell viability

Figure 5 shows the results of the direct TS treatment of HeLa cells. The initial concentration of the cells was approximately 5×10^5 cells/ml in 5 ml of PBS. Comparison of WE and WS systems [Fig. 5(a)] shows that similar cytotoxic effect of $\sim 50\%$ – 60% was achieved after 10 min of plasma exposure

in both systems. In all experiments, cell viability decreased with increasing exposure time and discharge power. The maximal cytotoxicity of 94% was observed with frequency of 4 kHz and 20 min exposure time and [Fig. 5(b)].

Direct exposure of the cells to the TS discharge was compared with the indirect exposure of the cells to the TS activated gas flow (30% O_2 in N_2 , 0.5 l/min) supplied via syringe needle toward the solution of cells. The cells with the same initial concentration of 5×10^5 cells/ml were placed in well plates, each well containing 100 μ l PBS to prevent cells from drying. Figure 6 shows the viability of Vero and HeLa cells indirectly exposed to the plasma for 2 and 4 min after 4 and 24 h of subsequent incubation. The incubation is the time interval the cells were allowed to grow in an incubator after the plasma exposure to enter to the log phase. After that, the cells were detached, resuspended in PBS, and their number determined by propidium iodide flow cytometry. As the figure shows, the total cytotoxic effect of indirect exposure was much smaller compared to the direct exposure. The cytotoxic effect increased with the treatment time, where after 4 min of plasma exposure and 4 h of subsequent incubation 25% of both HeLa and Vero cells were found dead [Fig. 6(a)]. While for HeLa cells the cytotoxic effect observed after 4 and 24 h of incubation remained relatively stable [Fig. 6(b)], in the case of Vero cells the cytotoxic effect was significantly attenuated with prolongation of the incubation period to 24 h. Lack of dead cells after 24 h

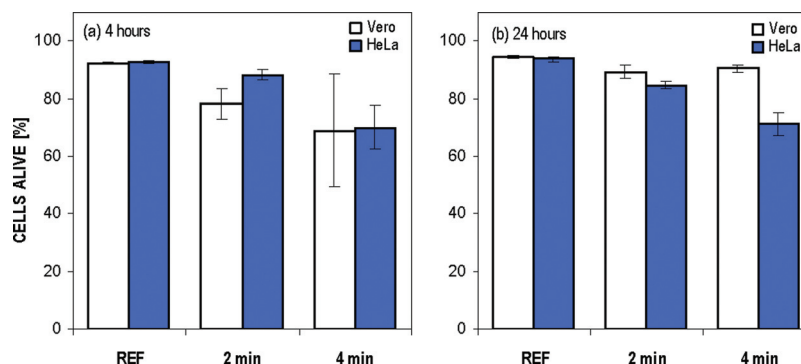


FIG. 6. Viability of **HeLa** and **Vero** line cells after indirect exposure to the TS and 4 h (a) vs 24 h (b) incubation time [cells in PBS, sample volume 100 μ l, applied voltage 12.5 kV, frequency ~ 2 kHz].

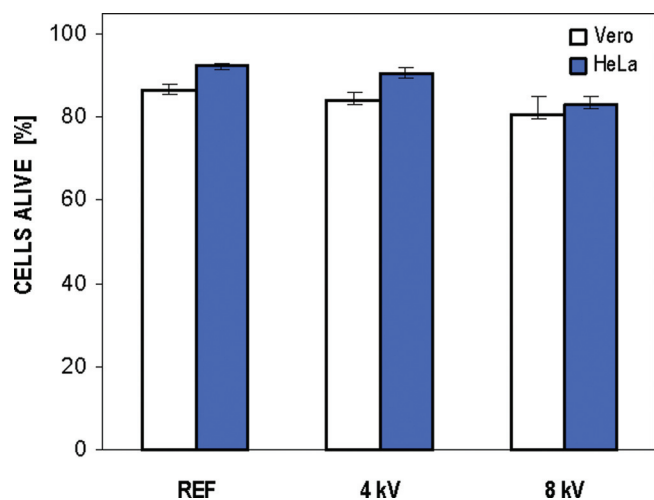


Fig. 7. Viability of Vero and HeLa cells after exposure to the PJ [cells in PBS, sample volume 100 μ l, frequency 4 kHz, exposure time 4 min, incubation 24 h].

despite apoptosis activation identified after 4 h can be explained by fast structural disintegration of cells. The result indicates that the cancerous cells can be selectively targeted and killed as they are more sensitive to the plasma exposure, while normal cells are more resistant to external injuries and more easily able to repair eventual damages.

A similar test of cytotoxicity was performed also with the PJ system. Figure 7 shows the results for Vero and HeLa cells exposed to the PJ for 4 min at two different applied voltages followed by 24 h of incubation. Also, in this experiment, the cells of the same initial concentration of 5×10^5 cells/ml were located in well plates containing 100 μ l PBS to prevent them from drying. After plasma exposure 1 ml of cell culture medium was added to the sample. The cells were treated without culture medium because for the PJ exposure of 1 ml culture medium no effects on viability were observed. The cytotoxic effect of the PJ system in the presented conditions was less than 10%, i.e., smaller than even compared with the results achieved with the indirect TS exposure.

2. Cell apoptosis

In order to probe the cell behavior before their dead, the test of cell apoptosis was performed. The apoptosis was analyzed by apoptotic assay utilizing bivariate staining analysis

by Annexin V-FITC and propidium iodide. Annexin V-FITC was used to identify the preapoptotic and apoptotic behavior, while propidium iodide was used to distinguish between live and dead cells. Figure 8 shows the results of the test performed on HeLa cells with indirect TS plasma exposure and for different incubation times. The analysis of the cells exposed to plasma and incubated for 4 h showed the number of cells that became apoptotic (27%). The analysis of the cells incubated for 24 h showed apoptotic cells disappearing from cell culture due to high disintegration of their structures and the corresponding increase of dead cells (32%) as a result of defective function of reparatory mechanisms in cancerous cells. Nonaffected cells or the remaining cells are able to proliferate, especially in the case of cancerous cells where proliferation is very intense. Also, depending on the moment of the cell cycle, some cells can trigger apoptosis, while others are not affected (especially in quiescent phase of cell cycle).

Figure 9 shows results for Vero cells obtained with indirect TS plasma exposure in similar conditions. The results show that 4 h after the exposure, a significant number of Vero cells were also determined as apoptotic (23%). However, with 24 h after the plasma exposure, the apoptotic effect vanished, values being similar with the reference, suggesting implication of an identification and reparation mechanism which decreased the negative impact of the plasma exposure on this type of normal cells. Compared with HeLa cells, Vero cells are less sensitive to plasma exposure and the occurrence of small number of dead cells after 24 h suggests that the part of Vero cells that were damaged by plasma were eliminated while a fraction of cells followed reparatory mechanisms. In normal cells, the proliferation is strictly controlled and if an error occurs the cell is halted and verified. After verification, if the error can be repaired then it will be repaired, if not, the cell is directed to apoptosis.

3. Cell cycle analysis

The cell cycle is a strictly controlled series of events in a mother cell leading to its division and duplication in two daughter cells. The cycle can be divided into three periods: interphase, the mitotic (M) phase, and cytokinesis. Cell cycle checkpoints are used by the cell to monitor and regulate the progress of the cell cycle. The main cell checkpoints are G_0/G_1 (ensures that everything is ready for DNA synthesis), S

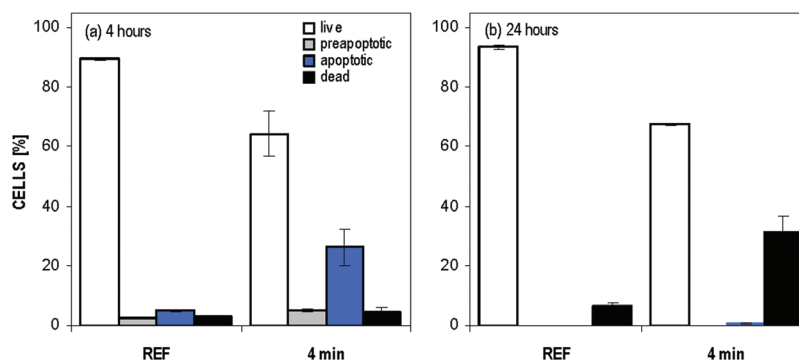


Fig. 8. Percentage distribution of the live, preapoptotic, apoptotic, and dead HeLa cells after indirect exposure to the TS and 4 h (a) and 24 h (b) of incubation [cells in PBS, sample volume 100 μ l, applied voltage, 12.5 kV, frequency \sim 2 kHz, exposure time 4 min].

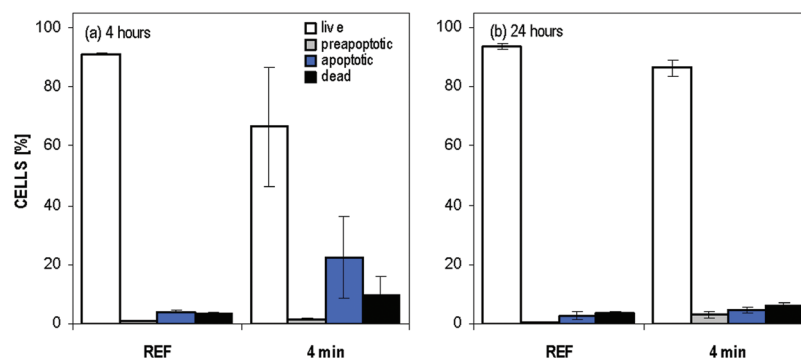


FIG. 9. Percentage distribution of live, preapoptotic, apoptotic, and dead Vero cells after indirect exposure to the TS and 4 h (a) and 24 h (b) of incubation [cells in PBS, sample volume 100 μ l, applied voltage, 12.5 kV, frequency \sim 2 kHz, exposure time 4 min].

(synthesis, duplication of chromosomes), G_2/M (ensures that everything is ready to enter the mitosis phase and divide), and M (ensures that the cell is ready to complete cell division). If a cell does not meet quality standards to pass through any checkpoint, then the cell cycle is stopped and cell is directed to apoptosis. The analysis of the cell viability and apoptotic behavior induced by plasma exposure was supplemented by the analysis of the cell cycle. The analysis of the cell cycle distribution was performed 24 h after plasma exposure to the PJ. The results of the analysis are presented in Fig. 10.

The results [Fig. 10(a)] show that in the case of Vero cells the plasma was responsible for the induction of a block in G_2/M stage and perturbation of cell cycle progression. The occurrence of G_2/M block, justified by a higher frequency of the cells in G_2/M stage compared to the reference, indicates the induction of DNA lesions by the plasma that have to be repaired before the cells pass to mitosis. The results on apoptosis suggested a fraction of cells seriously damaged by plasma were eliminated while a fraction of cells were in G_0 phase (and reactivated for proliferation) and few other fractions of cells (with minor errors) followed reparatory mechanism. The unreparable cells were directed to apoptosis and finally to death.

On the other hand, the impact of the plasma on progression of cell cycle in HeLa cells has determined a block in G_0/G_1 stage [Fig. 10(b)] and of frequency in G_2/M stage,

explained by the occurrence of G_0/G_1 block. Due to high proliferation rate, HeLa cells are more sensitive to plasma because a higher number of cells are in S phase. Overall damage impact is higher and prolonged in time. Not all damages occur immediately after plasma exposure but could be generated by secondary metabolites or other mechanisms.

E. Effects on biomolecules

The TS in WE and WS systems and the PJ were also applied for the treatment of various biomolecules normally present inside the cells (DNA and protein).

Figure 11 shows the effect of the TS operated in WE system on the solution of DNA. The analysis by UV spectrometry [Fig. 11(a)] showed the increase of the absorbance of the solution that corresponds to the fragmentation of total DNA molecules, where smaller fragments are responsible for higher absorbance. The effect of plasma exposure on DNA increased with the applied voltage amplitude and exposure time. The UV spectroscopic analysis was supplemented by fluorometric analysis of 1140 bp amplicons. As Fig. 11(b) shows, the average fluorescence of the exposed samples was lower compared to the reference sample. With the known affinity of SYBR Green for double stranded DNA,⁸² the registered decrease in fluorescence could be linked to the DNA denaturation with the occurrence of single stranded fragments or to the DNA degradation, leading to a decrease in the number of fluorochrome binding sites.

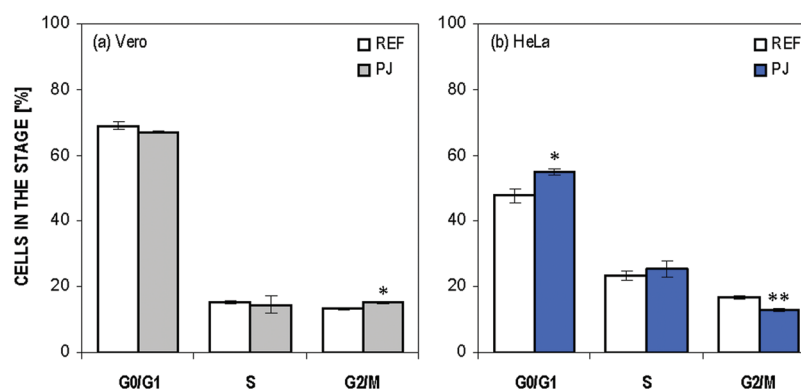


FIG. 10. Cell cycle analysis of Vero (a) and HeLa (b) cells after exposure to the PJ [applied voltage 4 kV, frequency 4 kHz, exposure time 4 min, incubation time 24 h]. The coefficient of variation of the peaks was $<8\%$. * $p < 0.05$; ** $p < 0.01$ by Student's test.

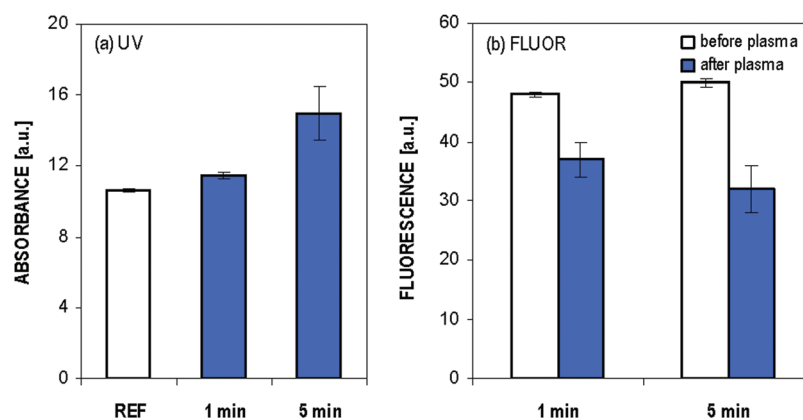


FIG. 11. Analysis of DNA after plasma exposure in the WE TS system analyzed by UV absorption spectroscopy (a) and 1140 bp amplicon fluorescence (b) [9 ng/ μ l of DNA in 2 ml of DI water, solution flow rate 5 ml/min].

BSA was used as a model protein to be exposed to the TS and the PJ systems. Several exposure times (3, 5, and 10 min) and repetition frequencies of driving voltage pulses were investigated in the PJ system, while effect of the applied voltage (15, 18 kV) and exposure time was investigated for the TS systems. Figure 12(a) shows that the concentration of BSA in the TS WS system decreased with the applied voltage. The voltage 0 kV refers to the solution supplied through the system without discharge application. The results show that the concentration of BSA decreased by 47% after 6 min exposure with 18 kV. The identical test was also performed in the WE system, with a slightly stronger effect observed.

Figure 12(b) shows treatment of BSA solution performed in the PJ system. With plasma exposure of 10 min, high voltage pulses amplitude 8 kV, and frequency 2 kHz, the concentration of BSA decreased only within a few percentage. The decrease of the concentration corresponds to the protein gradual unfolding during plasma treatment. The effect was reported by Takai,^{19,20} where plasma treatment inactivated lysozyme, a model protein, in the aqueous solution, which was accompanied by a conformational change and increase of molecular weight. Furthermore, the lysozyme structural modification was affected by the pH value of the solution.

IV. SUMMARY AND CONCLUSIONS

Self-pulsing DC TS discharge operated in air and pulsed DBD PJ operated in helium in contact with water solutions were used for the treatment of bacteria (*E. coli*), mammalian cells (Vero and HeLa line), and selected biomolecules (DNA and protein). Direct exposure of biological structures to the TS in WE and WS systems were compared with indirect exposure to the TS activated gas flow and to the effect of pulsed He DBD plasma jet.

The two TS systems of direct exposure showed similar chemical effects, water solution acidification, and comparable concentrations of RONS generated in water solutions, which were by one order of magnitude higher than concentrations of species generated by the PJ.

The TS systems showed strong bactericidal effects, stronger in nonbuffered (3–5 log) than in buffered solutions (1–2 log), as well as cytotoxic effects on mammalian cells. Cytotoxicity increased with treatment time and discharge power in both TS and PJ systems. The maximum of 94% was found with frequency of 4 kHz and 20 min exposure time in the TS WS system. Small concentrations of active species generated in water solutions by the PJ resulted in relatively weak bactericidal activity (<1 log reduction) and

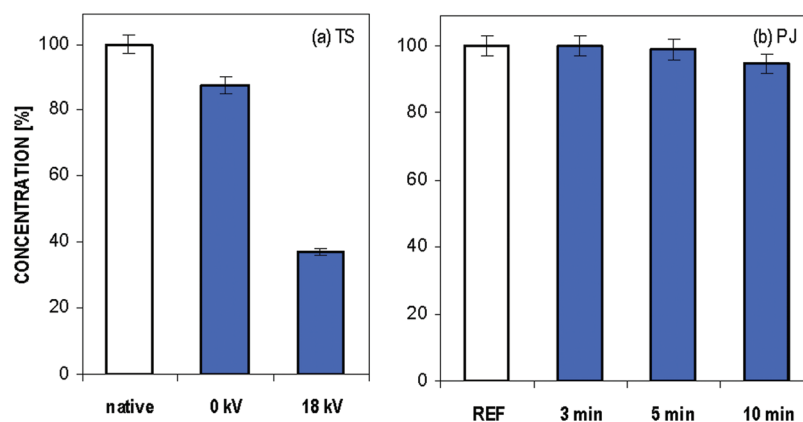


FIG. 12. Concentration of BSA in water solutions after plasma exposure to the TS WS system (a) [1 mg/ml of BSA in 3 ml of DI, solution flow rate 0.5 ml/min, exposure time 6 min] and to the PJ (b) [1 mg/ml of BSA in 4 ml of DI, applied voltage 8 kV, frequency 2 kHz].

cytotoxic effects on cells (<10%) compared with the TS direct exposure. The effect of the PJ was also smaller when compared with the indirect exposure to TS plasma. The results showed the discharges induced a cytotoxic effect on both normal and cancerous cells with similar result observed 4 h after plasma. However, 24 h after exposure, the cytotoxic effect was persistent only for HeLa cells, while the effect on Vero cells decreased. This suggests the plasma can selectively target and kill cancerous cells, while normal cells can effectively recover after the exposure. The cytotoxic effect was induced by activation of apoptotic mechanism, where the speed of the apoptosis induction was dependent on the characteristics of the discharges. In case of HeLa cells, the apoptotic cell cultures initially observed 4 h after plasma exposure were found dead 24 h after plasma exposure. The cell cycle analysis showed cell cycle block in G₂/M stage for normal cells, and in G₀/G₁ for cancerous one. The results of viability, apoptosis, and cell cycle clearly show the plasma can selectively target cancerous cells, which is very important for possible future development of new plasma therapeutic strategies in biomedicine.

The treatment of various biomolecules was also investigated to demonstrate the potential of plasma for successful fragmentation of DNA and denaturation of protein. The denaturation/degradation effect of DNA molecules was observed both on big molecules such as tDNA, as well as on short fragments. The denaturation of protein increased with the discharge power and exposure time up to 40%–50% in maximum with the TS system compared with only up to 10% in case of the PJ.

Our comparisons of the air TS discharge and the He PJ show that the chemical, bactericidal, cytotoxic, fragmentation, and denaturation effects are stronger in the air plasma of the TS than in He plasma jet and this is dominantly due to production of larger RONS concentrations in air TS plasma. Despite He plasma jets are very convenient for localized treatments and their main advantage is easy operation, little risk of arcing, and that the active plasma can be blown out from the interelectrode region to the target, the air plasmas demonstrate stronger biologically relevant effects, as shown here. The stronger formation of RONS, direct contact of the discharge with the liquid solution and therefore a better transport of the gas-phase active species generated by the air discharge into a water solution seem to be the key factors in plasma biomedical treatments. In our comparison, even indirect exposures to TS air plasma activated gas flow resulted in stronger effects than direct treatment by the He plasma jet, which further demonstrates the dominant role of RONS as key plasma agents. These results successfully demonstrated a great potential of the air self-pulsing TS discharge as an efficient tool for biomedical applications that is applicable in most settings, perhaps except direct *in vivo* tissue treatment.

ACKNOWLEDGMENTS

This work was supported by Slovak Research and Development Agency SK-RO-0024-12 and APVV 0134-12 grants, Slovak Grant Agency VEGA 1/0918/15 grant,

CNCS—UEFISCDI (Romania) through the joint Romanian-Slovak Cooperation Program, and COST Action TD1208—Electrical Discharges with Liquids for Future Applications.

- ¹A. Fridman and G. Friedman, *Plasma Medicine* (Wiley, New York, 2013).
- ²*Plasma for Bio-Decontamination, Medicine and Food Security, NATO Science for Peace and Security Series A: Chemistry and Biology*, edited by Z. Machala, K. Hensel, and Y. Akishev (Springer, New York, 2012).
- ³Th. von Woedtke, S. Reuter, K. Masur, and K.-D. Weltmann, *Phys. Rep.* **530**, 291 (2013).
- ⁴*Plasma Medicine: Applications of Low-Temperature Gas Plasmas in Medicine and Biology*, edited by M. Laroussi (Cambridge University, Cambridge, 2012).
- ⁵S. Kalghatgi, C. M. Kelly, F. Cerchar, B. Torabi, O. Alekseev, and A. Fridman, *PLoS One* **6**, e16270 (2011).
- ⁶E. Stoffels, I. E. Kieft, and R. E. J. Sladek, *J. Phys. D: Appl. Phys.* **36**, 2908 (2003).
- ⁷I. E. Kieft, M. Kurdi, and E. Stoffels, *IEEE Trans. Plasma Sci.* **34**, 1331 (2006).
- ⁸C. A. Schmitt and S. W. Lowe, *J. Pathol.* **187**, 127 (1999).
- ⁹S. J. Kim, T. H. Chung, S. H. Bae, and S. H. Leem, *Appl. Phys. Lett.* **97**, 023702 (2010).
- ¹⁰J. Y. Kim, J. Ballato, P. Foy, T. Hawkins, Y. Wei, J. Li, and S. Kim, *Biosens. Bioelectron.* **28**, 333 (2011).
- ¹¹M. Keidar, R. Walk, A. Shashurin, P. Srinivasan, A. Sandler, S. Dasgupta, R. Ravi, R. Guerrero-Preston, and B. Trink, *Br. J. Cancer* **105**, 1295 (2011).
- ¹²L. I. Partecke *et al.*, *BMC Cancer* **12**, 473 (2012).
- ¹³O. Kylian, M. Hasiwa, D. Gilliland, and F. Rossi, *Plasma Processes Polym.* **5**, 26 (2008).
- ¹⁴Z. Machala, L. Chládková, and M. Pelach, *J. Phys. D: Appl. Phys.* **43**, 222001 (2010).
- ¹⁵T. T. Chung, N. Ning, J. W. Chu, D. B. Graves, E. Bartis, J. Seog, and G. S. Oehrlein, *Plasma Processes Polym.* **10**, 167 (2013).
- ¹⁶J.-W. Lackmann, E. Edengeiser, S. Schneider, J. Benedikt, M. Havenith, and J. E. Bandow, *Plasma Med.* **3**, 115 (2013).
- ¹⁷O. Kylian, H. Rauscher, D. Gilliland, F. Bretagnol, and F. Rossi, *J. Phys. D: Appl. Phys.* **41**, 095201 (2008).
- ¹⁸C. Bernard, A. Leduc, J. Barbeau, B. Saoudi, L. H. Yahia, and G. De Crescenzo, *J. Phys. D: Appl. Phys.* **39**, 3470 (2006).
- ¹⁹E. Takai, K. Kitano, J. Kuwabara, and K. Shiraki, *Plasma Processes Polym.* **9**, 77 (2012).
- ²⁰E. Takai, T. Kitamura, J. Kuwabara, S. Ikawa, S. Yoshizawa, K. Shiraki, H. Kawasaki, R. Arakawa, and K. Kitano, *J. Phys. D: Appl. Phys.* **47**, 285403 (2014).
- ²¹X. T. Deng, J. J. Shi, and M. G. Kong, *J. Appl. Phys.* **101**, 074701 (2007).
- ²²A. Mizuno and S. Katsura, *J. Biol. Phys.* **28**, 587 (2002).
- ²³S. Lazović, D. Maletić, A. Leskovic, J. Filipović, N. Puać, G. Malović, G. Joksić, and Z. Lj. Petrović, *Appl. Phys. Lett.* **105**, 124101 (2014).
- ²⁴X. Han, W. A. Cantrell, E. E. Escobar, and S. Ptasińska, *Eur. Phys. J. D* **68**, 46 (2014).
- ²⁵D. O'Connell, L. J. Cox, W. B. Hyland, S. J. McMahon, S. Reuter, W. G. Graham, T. Gans, and F. J. Currell, *Appl. Phys. Lett.* **98**, 043701 (2011).
- ²⁶M. Miller, K. Foy, and P. Kaumaya, *Discovery Med.* **15**, 166 (2013).
- ²⁷D. B. Graves, *Plasma Processes Polym.* **11**, 1120 (2014).
- ²⁸S. Arndt, E. Wacker, Y. Li, T. Shimizu, H. Thomas, G. Morfill, S. Karrer, J. Zimmermann, and A. Bosserhoff, *Exp. Dermatol.* **22**, 284 (2013).
- ²⁹J. Chang *et al.*, *PLoS One* **9**, e92198 (2014).
- ³⁰S. Kalghatgi *et al.*, "Mechanism of Induction of Apoptosis in Melanoma Cancer Cells by Non-Thermal Plasma," in *36th IEEE International Conference on Plasma Science (ICOPS)*, San Diego, CA, 29th May–4th Jun 2009 (IEEE).
- ³¹K. Ninomiya, T. Ishijima, M. Imamura, T. Yamahara, H. Enomoto, K. Takahashi, Y. Tanaka, Y. Uesugi, and N. Shimizu, *J. Phys. D: Appl. Phys.* **46**, 425401 (2013).
- ³²M. Thiyagarajan, H. Anderson, and X. F. Gonzales, *Biotechnol. Bioeng.* **111**, 565 (2014).
- ³³O. Volotskova, T. S. Hawley, M. A. Stepp, and M. Keidar, *Sci. Rep.* **2**, 636 (2012).
- ³⁴X. Yan *et al.*, *IEEE Trans. Plasma Sci.* **38**, 2451 (2010).

- ³⁵Y. Ma, C. S. Ha, S. W. Hwang, H. J. Lee, G. C. Kim, K. W. Lee, and K. Song, *PLoS One* **9**, e91947 (2014).
- ³⁶R. Guerrero-Preston *et al.*, *Int. J. Mol. Med.* **34**, 941 (2014).
- ³⁷M. Keidar, A. Shashurin, O. Volotskova, M. A. Stepp, P. Srinivasan, A. Sandler, and B. Trink, *Phys. Plasmas* **20**, 057101 (2013).
- ³⁸W. Murphy, C. Carroll, and M. Keidar, *J. Phys. D: Appl. Phys.* **47**, 472001 (2014).
- ³⁹M. Naciri, D. Dowling, and M. Al-Rubeai, *Plasma Processes Polym.* **11**, 391 (2014).
- ⁴⁰M. G. Kong, M. Keidar, and K. Ostrikov, *J. Phys. D: Appl. Phys.* **44**, 174018 (2011).
- ⁴¹V. Miller, A. Lin, G. Fridman, D. Dobrynin, and A. Fridman, *Plasma Processes Polym.* **11**, 1193 (2014).
- ⁴²G. Collet, E. Robert, A. Lenoir, M. Vandamme, T. Darny, S. Dozias, C. Kieda, and J.-M. Pouvesle, *Plasma Sources Sci. Technol.* **23**, 012005 (2014).
- ⁴³J. Schlegel, J. Koritzer, and V. Boxhammer, *Clin. Plasma Med.* **1**, 2 (2013).
- ⁴⁴X. Cheng *et al.*, *J. Phys. D: Appl. Phys.* **47**, 335402 (2014).
- ⁴⁵L. Brullé *et al.*, *PLoS One* **7**, e52653 (2012).
- ⁴⁶J. S. Chang, P. A. Lawless, and T. Yamamoto, *IEEE Trans. Plasma Sci.* **19**, 1152 (1991).
- ⁴⁷U. Kogelschatz, *Plasma Chem. Plasma Process.* **23**, 1 (2003).
- ⁴⁸D. B. Graves, *J. Phys. D: Appl. Phys.* **45**, 263001 (2012).
- ⁴⁹D. B. Graves, *Clin. Plasma Med.* **2**, 38 (2014).
- ⁵⁰M. Naitali, J.-M. Herry, E. Hnatiuc, G. Kamgang, and J.-L. Brisset, *Plasma Chem. Plasma Process.* **32**, 675 (2012).
- ⁵¹M. J. Traylor, M. J. Pavlovich, S. Karim, P. Hait, Y. Sakiyama, D. S. Clark, and D. B. Graves, *J. Phys. D: Appl. Phys.* **44**, 472001 (2011).
- ⁵²T. A. Reiter, *Redox Rep.* **11**, 194 (2006).
- ⁵³E. Marode, A. Goldman, and M. Goldman, *High pressure discharge as a trigger for pollution control in Non-Thermal Plasma Techniques for Pollution Control*, NATO ASI Series, Part A, edited by B. M. Penetrante and S. E. Schultheis (Springer, New York, 1993), pp. 167–190.
- ⁵⁴R. Morrow and J. J. Lowke, *J. Phys. D: Appl. Phys.* **30**, 614 (1997).
- ⁵⁵Z. Machala, M. Morvová, E. Marode, and I. Morva, *J. Phys. D: Appl. Phys.* **33**, 3198 (2000).
- ⁵⁶X. Lu, M. Laroussi, and V. Puech, *Plasma Sources Sci. Technol.* **21**, 034005 (2012).
- ⁵⁷E. Robert *et al.*, *Clin. Plasma Med.* **1**, 8 (2013).
- ⁵⁸Z. Xiong, E. Robert, V. Sarron, J.-M. Pouvesle, and M. J. Kushner, *J. Phys. D: Appl. Phys.* **46**, 155203 (2013).
- ⁵⁹F. Pechereau, J. Jánský, and A. Bourdon, *Plasma Sources Sci. Technol.* **21**, 055011 (2012).
- ⁶⁰S. Lazović *et al.*, *New J. Phys.* **12**, 083037 (2010).
- ⁶¹X. Yan, Z. L. Xiong, F. Zou, S. S. Zhao, X. P. Lu, G. X. Yang, G. Y. He, and K. Ostrikov, *Plasma Processes Polym.* **9**, 59 (2012).
- ⁶²J. Heinlin, G. Morfill, M. Landthaler, W. Stolz, G. Isbary, J. L. Zimmermann, T. Shimizu, and S. Karrer, *J. Dtsch. Dermatol. Ges.* **8**, 968 (2010).
- ⁶³K.-D. Weltmann, K. Fricke, M. Stieber, R. Brandenburg, T. von Woedtke, and U. Schnabel, *IEEE Trans. Plasma Sci.* **40**, 2963 (2012).
- ⁶⁴A. Nastuta, V. Pohoata, and I. Topala, *J. Appl. Phys.* **113**, 183302 (2013).
- ⁶⁵J. Lademann *et al.*, *J. Biomed. Opt.* **14**, 054025 (2009).
- ⁶⁶M. Vandamme *et al.*, *Int. J. Cancer* **130**, 2185 (2012).
- ⁶⁷F. Utsumi *et al.*, *PLoS One* **8**, e81576 (2013).
- ⁶⁸J. Y. Kim, S. O. Kim, Y. Z. Wei, and J. H. Li, *Appl. Phys. Lett.* **96**, 203701 (2010).
- ⁶⁹M. Janda, V. Martišovits, and Z. Machala, *Plasma Sources Sci. Technol.* **20**, 035015 (2011).
- ⁷⁰M. Janda, Z. Machala, A. Niklová, and V. Martišovits, *Plasma Sources Sci. Technol.* **21**, 045006 (2012).
- ⁷¹Z. Machala, B. Tarabová, K. Hensel, E. Špetliková, L. Šikurová, and P. Lukeš, *Plasma Processes Polym.* **10**, 649 (2013).
- ⁷²W. Strober, *Current Protocols in Immunology* (Wiley, New York, 2001), 21:3B:A.3B.1–A.3B.2.
- ⁷³Z. Machala, M. Janda, K. Hensel, I. Jedlovský, L. Leštinská, V. Foltin, V. Martišovits, and M. Morvová, *J. Mol. Spectrosc.* **243**, 194 (2007).
- ⁷⁴M. Janda, V. Martišovits, K. Hensel, L. Dvonč, and Z. Machala, *Plasma Sources Sci. Technol.* **23**, 065016 (2014).
- ⁷⁵I. Topala, N. Dumitrascu, and D. G. Dimitriu, *IEEE Trans. Plasma Sci.* **40**, 2811 (2012).
- ⁷⁶A. V. Nastuta, I. Topala, C. Grigoras, V. Pohoata, and G. Popa, *J. Phys. D: Appl. Phys.* **44**, 105204 (2011).
- ⁷⁷R. Jijie, V. Pohoata, and I. Topala, *Appl. Phys. Lett.* **101**, 144103 (2012).
- ⁷⁸M. Wertheimer, M. Ahlawat, B. Saoudi, and R. Kashyap, *Appl. Phys. Lett.* **100**, 201112 (2012).
- ⁷⁹I. Topala and M. Nagastu, *Appl. Phys. Lett.* **106**, 054105 (2015).
- ⁸⁰P. Lukeš, E. Doležalová, I. Sisrová, and M. Člupek, *Plasma Sources Sci. Technol.* **23**, 015019 (2014).
- ⁸¹J.-L. Brisset and E. Hnatiuc, *Plasma Chem. Plasma Process.* **32**, 655 (2012).
- ⁸²S. Giglio, P. T. Monis, and C. P. Saint, *Nucleic Acids Res.* **31**, e136 (2003).